BioMetals **17:** 217–223, 2004.

Molecular dynamics simulations of bovine lactoferricin: turning a helix into a sheet

Ning Zhou, D. Peter Tieleman & Hans J. Vogel*
Structural Biology Research Group, Department of Biological Sciences, University of Calgary, Calgary, AB T2N 1N4
**Author for correspondence (Tel: (403) 220-6006; Fax: (403) 289-9311; E-mail: vogel@ucalgary.ca)*

Abstract

Bovine lactoferricin is a 25-residue peptide that is excised through pepsin cleavage in the stomach from the intact 80 kDa bovine milk protein lactoferrin. This basic peptide contains a single disulfide crosslink and is considerably more active as an antimicrobial peptide than the intact protein. It has been suggested that the dramatic difference in potency is related to a change in the secondary and tertiary structure of this peptide, moving from a mixed α-helical β-strand region in the protein to an amphipathic twisted antiparallel β-sheet in the peptide. Here we have used equilibrium and restrained molecular dynamics calculations to compare the stability of the solution structure of the isolated peptide with that excised from the intact protein. Simulations were performed for fully solvated peptides in the absence and presence of 250 mM salt. Our results show that the peptide as released from the protein is relatively unstable, particularly in the absence of salt. However, even though the simulations extended over 60 nsecs, no interconversion could be observed between the crystal and solution structures, unless a relatively small directional force was exerted on the peptide. A pathway for the structural transition from a helical to a sheet structure was identified in this fashion.

Abbreviations: MD – molecular dynamics; DSSP – dictionary of secondary structure patterns; SPC – simple point charge; ACE – angiotensin-converting enzymes.

Introduction

Many major milk proteins can release bioactive peptides when they are activated by enzymatic proteolysis during gastrointestinal digestion or food processing (Meisel 1997, Meisel & Bockelmann 1999). The activated peptides can potentially modulate various physiological processes in the body, e.g. opioid peptides can influence intestinal absorption processes, ACE-inhibitory peptides have a hemodynamic action, while immunomodulating and antimicrobial peptides activate the immune system and kill microorganisms thereby protecting humans against infections. Antimicrobial peptides can also be released through proteolysis of various other food proteins (Pellegrini 2003). In most cases the beneficial effects of the bioactive peptides are masked when they are part of the parent protein. Typically the biological activity appears only upon release of the peptide by proteolysis. Such peptides hold great potential as nutraceuticals or functional food.

One of the best-studied examples of this peptide activating process is the release of the immunostimulating and antimicrobial peptide lactoferricin B from the bovine milk protein lactoferrin through treatment with pepsin at acidic pH. A little more then a decade ago Bellamy *et al.* (1992) reported that a 25-residue peptide derived from a highly cationic region near the N-terminus of bovine lactoferrin, had a markedly increased antimicrobial potency compared to the parent protein. The 'lactoferricin B' peptide was active against many gram-positive and gram-negative bac-

Supported by grants from the Canadian Institutes of Health Research. DPT and HJV are the recipients of Scholar and Scientist awards, respectively from the Alberta Heritage Foundation for Medical Research.

teria as well as fungi and protozoa, while displaying immunostimulating effects and maintaining a low hemolytic activity (for review, see, Wakabayashi *et al.* 2003). It has also been shown that the peptide has direct antiviral (Anderson *et al.* 2003) and antitumor (Eliassen *et al.* 2002, Roy *et al.* 2002) activities. Thus the lactoferricin B peptide has an impressive array of beneficial activities. Finally, Kuwata & coworkers (1998) have shown that lactoferricin B is formed through proteolysis in the stomach and that it can pass intact through the gut thus being able to exert its actions *in vivo*.

Many analogs of this peptide (FKCRRWQWRMK KLGAPSITCVRRAF) have been synthesized over the last decade and these studies have shown that the Trp6 and Trp8 residues as well as several of the cationic Arg residues were essential for the antimicrobial activity (Strøm *et al.* 2002, Vogel *et al.* 2002). The peptide has been shown to bind to the cytoplasmic membrane of bacterial cells in a parallel fashion (Schibli *et al.* 2002), but it is also capable of entering the cell thereby probably exerting its bactericidal activity (Haukland *et al.* 2001, Vogel *et al.* 2002). Hwang *et al.* (1998) have determined the structure of the peptide in aqueous solution by NMR methods. The peptide displayed a slightly twisted antiparallel β-sheet structure, which was markedly different from that found in the crystal structure of the intact protein. The overall beta-hairpin structural layout is stabilized by a single disulfide bond. This region in the crystal structure of the intact protein is characterized by an α-helix followed by a single β-strand (Moore *et al.* 1997). Based on these structural results it was suggested that the transition from a helix to an amphipathic β-sheet structure was crucial for the activation observed upon proteolytic release of the peptide (Hwang *et al.* 1998).

Here we present equilibrium molecular dynamics simulations starting from the NMR-determined solution structure of the lacteroferricin B peptide, as well as the structure of the same region excised out of the intact protein (Figure 1). This approach would allow us to assess the stability of this region in both structural extremes (Bonvin & van Gunsteren 2000). Simulations were also carried out with added salt as this has been shown to stabilize marginally stable protein and peptide structures in MD simulations (Ibragimova & Wade 1998). Subsequently restrained MD simulations were performed to force the transition from the crystal structure to the solution structure and study the process in detail.

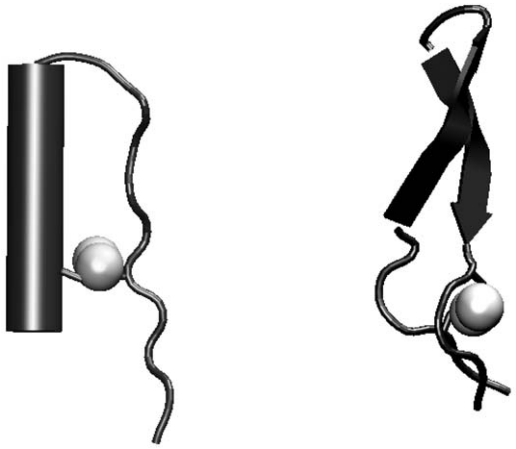

Fig. 1. Structure of the lactoferricin fragment taken from the crystal structure on the left and the structure from the solution NMR study on the right. The β-sheet and α-helical structure are indicated by arrows and cylinders respectively. The spheres highlight the two disulfide-linked Cys residues.

Methods

Structure files for lactoferricin B were obtained from the protein database entries 1LFC (NMR structures, Hwang *et al.* 1998) and 1BLF (crystal structure, Moore *et al.* 1997). In the case of the crystal structure residues 17–41 were excised without modification. The N- and C-terminal ends of both peptides contained the usual protonated amino and negatively charged carboxylate groups, consistent with their protonation state at physiological pH. The disulfide bond between Cys3 and Cys20 was maintained. Throughout this study the peptide was labeled as 1 through 25, corresponding to residues 17–41 in the intact bovine Lf. In the peptide taken from the crystal structure hydrogen atoms were added to the polar, charged and aromatic groups as required by GROMACS (Berendsen *et al.* 1995; Lindahl *et al.* 2001; http://www.gromacs.org). In the case of the NMR structure aliphatic hydrogens are treated using the standard united atom approach. All simulations were done under periodic boundary conditions. Four different systems were analyzed representing the NMR and crystal structures in aqueous solution in the presence or absence of salt (250 mM NaCl). Cubic simulation boxes contained a single isolated peptide placed in the centre and were completely filled with SPC water (Berendsen *et al.* 1981), using routine GROMACS procedures. To obtain overall neutrality 8 Cl^- ions were added in the system, randomly replacing water molecules. For the salt simulations an additional 23 Na^+ and 23 Cl^- ions

were added, which corresponds roughly to a 250 mM NaCl concentration in the simulation box. We chose a slightly higher than physiological salt concentration in order to influence protein stability, which has often been done. The size of a typical simulation box was 5.0 by 5.0 by 5.0 nm which, in addition to the peptide, contained approximately 4,900 water molecules, giving a total simulation size of 15,000 atoms. Using the GROMOS96 force field G43a2 (van Gunsteren *et al.* 1996) as implemented in GROMACS, simulations were done in steps of 2 femtosec with a cutoff for Vander Waals interactions of 1.4 nm and coulumbic interactions of 0.9 nm. Long-range electrostatic interactions were handled by using the particle mesh Ewald methodology (Essmann *et al.* 1995). Temperature (30 °C) and pressure (1 atm) were kept constant throughout by coupling to external baths (Berendsen *et al.* 1984). Coordinates and velocities were stored every ps for subsequent analysis. Each simulation was carried out on 2 Intel PIII processors (1 GHz), giving an approximate calculation time of 4.5 weeks to obtain a 20 ns trajectory.

Starting point for the simulations with harmonic restraints was the lactoferrin fragment from the crystal structure in 250 mM salt. In each simulation all non-hydrogen atoms of the starting structure were harmonically restrained to their coordinates in the NMR structure of the lactoferrin fragment in water after best-fitting the crystal structure and NMR structures on top of each other. Harmonic force constants ranging from 1 to 1000 kJ mol^{-1} nm^{-2} were used in simulations of up to 10 ns. The system for these restrained simulations consisted of a total of 14,912 atoms, 23 Na^{+}, 31 Cl^{-} and 4,851 water molecules. In this case nonbonded interactions were calculated using a twin range cutoff of 0.8/1.4 nm for both Coulomb and Van der Waals, combined with a reaction field with a dielectric constant of 59 for electrostatic interactions beyond 1.4 nm. This dielectric constant corresponds to that of SPC water. Otherwise similar simulation parameters were used as above in the non-restrained simulations.

Results

Figure 1 shows the structure of the peptide excised from the crystal structure on the left containing an α-helix and a β strand held together by a single disulfide bond. On the right the NMR structure determined in aqueous solution reveals a twisted antiparallel β-sheet

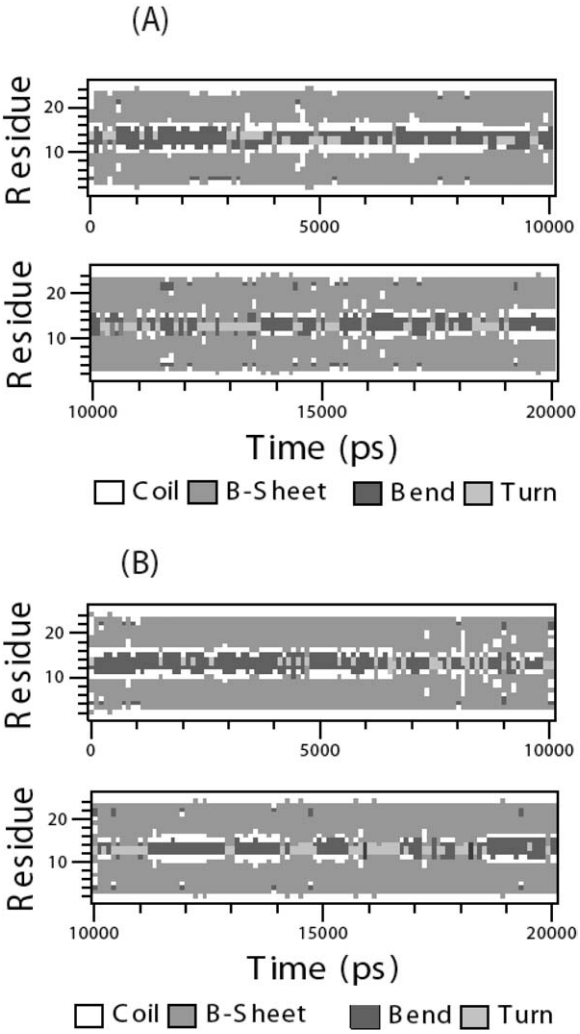

Fig. 2. Trajectories for the two simulations starting from the NMR solution structure in the absence (panel A) and presence (panel B) of salt (see Methods). The x-axis represent the time course, the y-axis gives the peptide sequence numbers. Different secondary structure elements are indicated by different gray scales as indicated. Structure elements are assigned using the DSSP package in Gromacs (Kabsch and Sander 1983).

and a loop structure resembling a β-bend. In our initial MD simulations, these were used as the starting structures and simulations were extended to 20 nsecs in all instances. The results obtained for the secondary structure are summarized in Figures 2 and 3 for the NMR and crystal structures respectively, with panel A showing the simulation without added salt and panel B with 250 mM NaCl. Different secondary structure elements are represented by different gray scales in the figures. Inspection of the two simulations starting with the NMR structure, showed virtually no changes. The

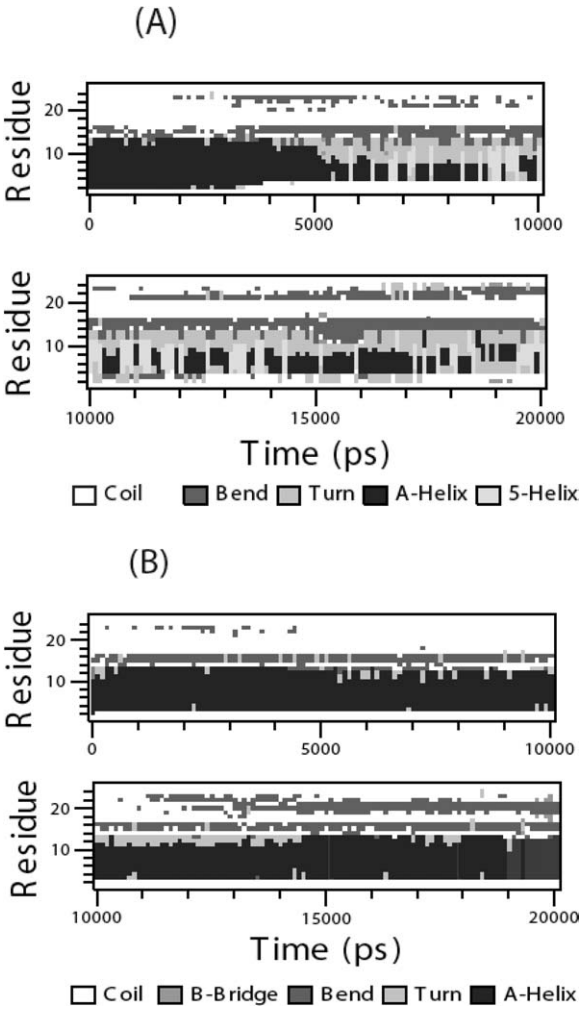

Fig. 3. Trajectories for the two simulations starting from the crystal structure in the absence (panel A) and presence of salt (panel B). For further details see legend of Figure 2.

β-strands stay in position throughout the simulations and although the central loop is occasionally broken and replaced by various turn and coil structures, it always rapidly refolds. Both extreme ends of the peptides maintain their poorly structured nature. Overall it appears that the loop structures is somewhat more stable in the presence of salt, but otherwise there does not appear to be much difference between the two distinct simulations of the solution structure.

A somewhat different picture was obtained for the two simulations starting from the crystal structure. In the presence of salt (Figure 3, panel B) the α-helical structure was largely maintained throughout the simulation, although between 9 and 15 nsecs the α-helix shortens from the loop side, but subsequently it returns to the original state. Some extra β-bend (but no β-sheet) structure is also formed near the C-terminal end that seems to persist. The helical structure in this simulation contained almost no 3_{10} or π-helical structures. The most drastic changes were observed for the simulation of the crystal structure in the absence of salt (Figure 3, panel A). Around 4 nsecs the helix starts to shorten from both ends being replaced largely by turn structures on the loop side and coil structures on the N-terminal side. The structure subsequently maintains an equilibrium between α-helical and π-helical structure for residues 4 to 9. The β-bend structure near the C-terminal end is again formed here. The loop structure seems to be relatively well maintained. Since large changes were observed here, this simulation was extended to 65 nsecs and it was observed that the loop structure and the C-terminal β-bend remained throughout while the helical structure reestablished itself at its original length after 25 nsecs for the remainder of the simulation (data not shown).

A characteristic difference between the NMR and crystal structures is the orientation of the two Trp residues in the peptide. In the NMR structure they are on the same sides of the amphipathic molecule, whereas they are on opposite sides in the crystal structure with Trp8 facing towards the solvent and Trp6 facing into the core of the protein. Bringing the two Trp to one side of the peptide is believed to be very important for the increase in antimicrobial activity (Hwang *et al.* 1998). In Figure 4 we show the radial distribution functions for the two Trp residues. The top panel, with the two NMR simulations shows that they remain at a very similar distance from each other in the course of the 20 nsec simulation. The distribution is much broader for the crystal structure simulation in the absence of salt, indicating motion of one Trp with respect to the other. This is consistent with the observed change in secondary and tertiary structure upon proteolytic release of the peptide from the intact protein.

Since no complete interchange between the two different structures could be obtained in non-restrained equilibrium MD simulations we decided to see if we could 'pull' the original structure towards the NMR solution structure using harmonic restraints (see Figures 5 and 6). The harmonic restraints force the crystal structure to adopt the solution structure of the isolated fragment. At the highest force constant of 1,000 kJ mol^{-1} nm^{-2} interconversion between the two structures is almost immediate; at two intermediate values of 25 kJ mol^{-1} nm^{-2} and 100 kJ mol^{-1} nm^{-2}

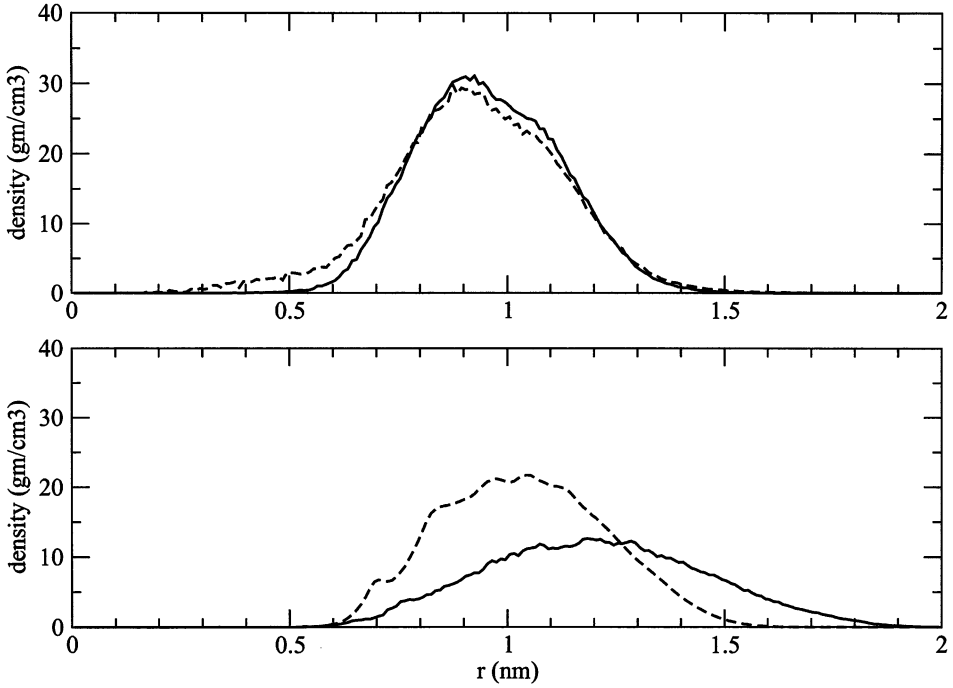

Fig. 4. Radial distribution functions showing the distance between the two Trp residues of bovine lactoferricin for the 20 ns simulations of the NMR structures (top) and the crystal structures (bottom). Solid lines represent simulations without salt, broken lines give the results for the simulations with 250 mM NaCl.

interconversion occurs on a timescale of 2.5 nsecs and 100 psecs respectively. For smaller force constants the starting structure, including the helical portion, is stable in 10 ns simulations (data not shown).

Figure 5 shows the conversion between the two extreme structures obtained with a force constant of 25 kJ mol^{-1} nm^{-2} (Figures 5A, C) and 100 kJ mol^{-1} nm^{-2} (Figures 5B, D). The total number of peptide-peptide hydrogen bonds very rapidly drops from ca. 15 to ca. 5 initially, and then slowly recovers as the peptide assumes its beta-sheet structure (Figures 5 A,B). The total number of hydrogen bonds between the peptide and solvent increases after the initial unfolding and then fluctuates slowly for the remainder of the simulations (Figures C,D). Figures 6A and 6B show the secondary structure of the peptide during each simulation. In both cases, the α-helix rapidly unfolds in the first couple of picoseconds. The most stable part of the structure is the loop near residues 11–14. After the α-helix has unfolded random coil structure dominates before the β-sheets start forming.

Discussion

The equilibrium MD simulations show that the solution structure of lactoferricin B is well maintained during the 20 ns simulations. The β-sheet structure is stable and also the loop structure does not break for any significant length of time (Figure 2). The stability of this structure might be explained by the fact that all hydrophobic residues are clustered on one face of the β-hairpin structure (Hwang *et al.* 1998). Nevertheless the seven positively charged sidechains are all on the opposite face of the sheet and this would tend to destabilize this structure. The presence of the salt stabilizes the structure, likely through contributing to shielding effects for the positively charged residues.

In the case of the peptide excised from the crystal structure, it is obvious that the helix is the least stable secondary structure element (Figure 3A). This is also clearly seen in the restrained simulations, where it disappears almost immediately (Figure 6), losing many intrapeptide hydrogen bonds (Figure 5). As the helical structure is broken, also the sidechains acquire greater flexibility (see Figure 4). In the crystal structure the positively charged residues are all on one face of the helix (Moore *et al.* 1997). This probably is a major

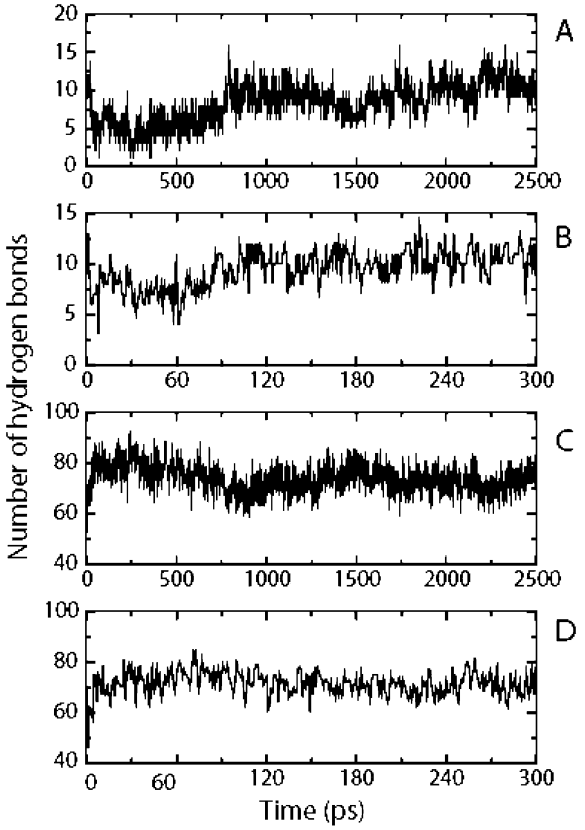

Fig. 5. Results obtained for the restrained simulations with applied forces of 25 and 100 kJ mol^{-1} nm^{-1}. Panels A and B show the number of hydrogen bonds in the peptide, while panels C and D show hydrogen bond formation with the solvent.

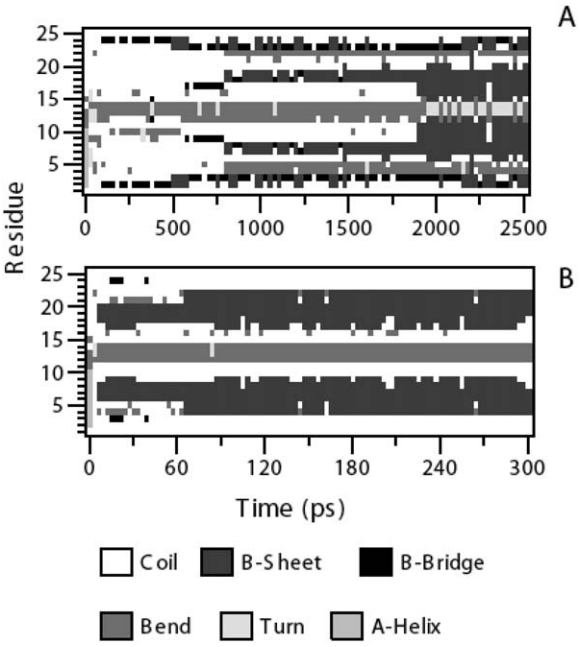

Fig. 6. Panels A and B show the secondary structure changes over the 2,500 ps and 300 ps respectively for the two different forces used. For explanation see also Figure 2 legend. See text for further explanation. A movie showing the conversion of the crystal structure into the solution structure can be viewed at http://moose.bio.ucalgary.ca, Gallery.

cause of its instability, when other stabilizing interactions with the remainder of the protein are missing. The effect of the added salt is quite dramatic in this case, the shielding afforded appears to stabilize the helix (Figure 3B).

Nevertheless, the helix unfolding never led to the formation of the antiparallel β-sheet even in an equilibrium simulation of 65 nsecs. Significantly the loop structure appears to be very stable in all the simulations reported here. Thus the peptide appears to be restrained by a disulfide on one end and a stable loop on the other end. Such behaviour has also been observed in earlier simulations and experimental studies of various β-hairpins (e.g. Ramirez-Alvardo *et al.* 1999, Bonvin & van Gunsteren 2000, Espinosa *et al.* 2001), which are the typical basic folding units for antiparallel β-sheet formation. These studies all draw attention to the stability of the loop and hydrophobic clustering as major driving forces for sheet formation, similar to what is seen in our simulations for the structural interconversion of lactoferricin B.

Although forcing the transition from the crystal structure to the solution structure by applying harmonic restraints is somewhat artificial, it nonetheless shows some interesting details of the conformational change in the peptide that occurs in the stomach after digestion of lactoferrin. The use of different force constants enables an estimate of the potential artifacts introduced by this method. The path between the two structures is very similar with either a force constant of 25 or 100 kJ mol^{-1} nm^{-2}, although the rate at which the structure changes is much slower at the lower force constant. This suggests that the path between the two structures is physically quite reasonable, and is likely to be the same without artificial forces. The committing step appears to be the complete unfolding of the α-helix. Subsequently with both ends restrained by the loop and the disulfide linkage, the hydrophobic collapse and hydrogen-bonding interactions necessary for β-sheet formation can proceed. Overall our results show that the transition from the relatively unstable α-helix can lead to a more stable sheet structure for lactoferricin B in solution.

References

Anderson JM, Jensen H, Gutteberg TJ. 2003 Lactoferrin and lactoferricin inhibit Herpes simplex 1 and 2 infection and exhibit synergy with acyclovir. *Antiviral Res* **58**, 209–215.

Bellamy W, Takase M, Yamauchi K, Wakabayashi H, Kawase K, Tomita H. 1992 Identification of the bactericidal domain of lactoferrin. *Biochim Biophys Acta* **1121**, 130–136.

Berendsen HJC, Postma JPM, van Gunsteren WF, Hermans J. 1981 Interaction models for water in relation to protein hydration. In Intermolecular Forces pub. Reidel, Dordrecht, 331–342.

Berendsen HJC, Postma JPM, van Gunsteren WF, DiNola A, Haak JR. 1984 Molecular dynamics with coupling to an external bath. *J Chem Phys* **81**, 3684–3690.

Berendsen HJC, van der Spoel D, van Drunen R. 1995 Gromacs a message-passing parallel molecular dynamics implementation. *Comp Phys Comm* **91**, 43–56.

Bonvin AM, van Gunsteren WF. 2000 Beta-hairpin stability and folding: molecular dynamics simulations of the first beta-hairpin of tendamistat. *J Mol Biol* **296**, 255–268.

Eliassen LJ, Berge G, Sveinbjornsson B, Svendsen JS, Vorland LH, Reldal O. 2002 Evidence for a direct antitumor mechanism of action of bovine lactoferricin. *Anticancer Res* **22**, 2703–2710.

Espinosa JF, Munoz V, Gellman SH. 2001 Interplay between hydrophobic clustering and loop propensity in beta hairpin formation. *J Mol Biol* **306**, 397–402.

Essmann U, Perera L, Berkowitz ML, Darden T, Lee H, Pedersen LG. 1995 A smooth particle mesh ewald method. *J Chem Phys* **103**, 8577–8593.

Haukland HH, Ulvatne H, Sandvik K, Vorland LH. 2001 The antimicrobial peptides lactoferricin B and magainin 2 crossover the bacterial cytoplasmic membrane and reside in its cytoplasm. *FEBS Lett* **508**, 389–393.

Hwang PM, Zhou N, Shan X, Arrowsmith CH, Vogel HJ. 1998 Three-dimensional solution structure of lactoferricin B, an antimicrobial peptide derived from bovine lactoferrin. *Biochemistry* **37**, 4288–4298.

Ibragimova GT, Wade RC. 1998 Importance of explicit salt ions for protein stability in molecular dynamics simulations. *Biophys J* **74**, 2906–2911.

Kabsch W, Sander C. 1983 Dictionary of protein secondary structure: pattern recognition of hydrogen bonding and geometrical features. *Biopolym* **22**, 2577–2637.

Kuwata H, Yip TT, Tomita M, Hutchens TW. 1998 Direct evidence of the generation in human stomach of an antimicrobial peptide domain (lactoferricin) from ingested lactoferrin. *Biochim Biophys Acta* **1429**, 129–141.

Lindahl E, Hess B, van der Spoel W. 2001 Gromacs 3.0: a package for molecular simulation and trajectory analysis. *J Mol Model* **7**, 306–317.

Meisel H, Bockelman W. 1999 Bioactive peptides encrypted in milk proteins: proteolytic activation and thropho-functional properties. *Antonie van Leeuwenhoek* **76**, 207–215.

Meisel H. 1997 Biochemical properties of regulatory peptides derived from milk proteins. *Biopolymers* **43**, 119–128.

Moore SA, Andersson BF, Groom CR, Haridas EM, Baker EN. 1997. Three-dimensional structure of diferric bovine lactoferrin at 2.8 Å resolution. *J Mol Biol* **274**, 222–236.

Pellegrini A. 2003 Antimicrobial peptides from food proteins. *Curr Pharm Des* **9**, 1225–1238.

Ramirez-Alvardo M, Kortemme T, Blanco FJ, Serrano L. 1999 Beta-hairpin and beta sheet formation in designed linear peptides. *Biorg Med Chem* **7**, 93–103.

Roy MK, Kuwabara H, Hara K, Watanabe Y, Tamai Y. 2002 Peptides from the N-terminal end of bovine lactoferrin induce apoptosis in human leukemic (HL60) cells. *J Dairy Sci* **85**, 2065–2074.

Schibli DJ, Epand RF, Vogel HJ, Epand RM. 2002 Tryptophan-rich antimicrobial peptides: comparative properties and membrane interactions. *Biochem Cell Biol* **80**, 667–677.

Strøm MB, Haug BE, Rekdal O, Skar ML, Stensen W, Svendsen JS. 2002 Important structural features of 15-residue lactoferricin derivatives and methods for improvement of antimicrobial activity. *Biochem Cell Biol* **80**, 65–74.

van Gunsteren WF, Kruger P, Billeter SR, Mark AE, Eising AA, Scott WRP, Huneberger PH, Tironi IG. 1996 Biomolecular simulation: the GROMOS96 mannual and user Guide. Biomos Hochschulverlag AG an der ETH Zurich, Groningen.

Vogel HJ, Schibli DJ, Jing W, Lohmeier-Vogel EM, Epand RF, Epand RM. 2002 Towards a structure function analysis of bovine lactoferricin and related tryptophan and arginine-containing peptides. *Biochem Cell Biol* **80**, 49–63.

Wakabayashi H, Takase M, Tomita M. 2003. Lactoferricin derived from milk protein lactoferrin. *Curr Pharm Des* **9**, 1277–1287.